JOURNAL OF GEOPHYSICAL RESEARCH, VOL. 112, B03S10, doi:10.1029/2005JB004200, 2007



# Slip rates on the Chelungpu and Chushiang thrust faults inferred from a deformed strath terrace along the Dungpuna river, west central Taiwan

Martine Simoes,[1,2,3] Jean Philippe Avouac,[1] and Yue-Gau Chen[4]

Received 1 December 2005; revised 29 June 2006; accepted 29 August 2006; published 9 February 2007.

[1] The Chelungpu fault produced the September 1999 $M_w$ = 7.6 Chi-Chi earthquake, central Taiwan. The shortening rate accommodated by this structure, integrated over several seismic cycles, and its contribution to crustal shortening across the Taiwanese range have remained unresolved. To address the issues, we focus our study on the Chelungpu and Chushiang thrust faults within the southernmost portion of the Chi-Chi rupture area. Structural measurements and available seismic profiles are used to infer the subsurface geometry of structures. The Chushiang and Chelungpu faults appear as two splay faults branching onto a common ramp that further north connects only to the Chelungpu surface trace. We survey a deformed strath terrace along the Dungpuna river, buried under a 11,540 ± 309 years old fill deposit. Given this age, the dip angles of the faults, and the vertical throw determined from the offset of the strath terrace across the surface fault traces, we estimate slip rates of 12.9 ± 4.8 and 2.9 ± 1.6 mm/yr on the Chelungpu and Chushiang faults, respectively. These yield a total shortening rate of 15.8 ± 5.1 mm/yr to be absorbed on their common decollement at depth. This total value is an upper bound for the slip rate on the Chelungpu fault further north, where the Chushiang fault disappears and transfers shortening to adjacent faults. Combining these results with the recently constrained shortening rate on the Changhua blind thrust reveals that all these frontal faults presently absorb most of the long-term horizontal shortening across the Taiwanese range. They thus stand as the major sources of seismic hazards in this heavily populated area. The return period of earthquakes similar to the Chi-Chi event over a ~80 km long stretch of the Western Foothills is estimated to be ~64 years. This value is an underestimate because it assumes that all the faults locked during the interseismic period slip only during such large events. Comparison with historical seismicity suggests that episodic aseismic deformation might also play a major role in accommodating shortening.

**Citation:** Simoes, M., J. P. Avouac, and Y.-G. Chen (2007), Slip rates on the Chelungpu and Chushiang thrust faults inferred from a deformed strath terrace along the Dungpuna river, west central Taiwan, *J. Geophys. Res.*, *112*, B03S10, doi:10.1029/2005JB004200.

## 1. Introduction

[2] Taiwan is located at the boundary between the Philippine Sea Plate and the Chinese continental margin, which converge at a rate of ~90 mm/yr in a NW-SE direction [*Sella et al.*, 2002] (Figure 1). A fraction of this convergence is absorbed by shortening across the Taiwanese range, which comprises the Central Range (CR) and the Western Foothills (WF). Several active faults, such as the Changhua blind thrust, the Chelungpu fault that broke during the 1999 Chi-Chi earthquake [*Ma et al.*, 1999], the Chushiang and the Shuangtung faults, have been recognized in the western frontal area [*Bonilla*, 1975, 1999; *H.-W. Chen et al.*, 2004; *Shyu et al.*, 2005; *Sung et al.*, 2000; *Tsai*, 1985] (Figures 2 and 3) and may all play an active role in accommodating this shortening. Interseismic strain measured from GPS data before the Chi-Chi earthquake [*Yu et al.*, 1997] shows that all these faults are locked, and that they probably root at depth beneath the range into a decollement that creeps at 27 to 45 mm/yr [*Dominguez et al.*, 2003; *Hsu et al.*, 2003; *Loevenbruck et al.*, 2001] (Figure 4). These rates, derived for a very short timescale of ~5 years, compare well with the 39.5–44.5 mm/yr shortening rate across the range recently proposed over the last 1.9 Myr based on the analysis of the foreland basin [*Simoes and Avouac*, 2006]. How this short-

[1]Tectonics Observatory, California Institute of Technology, Pasadena, California, USA.
[2]Laboratoire de Géologie, CNRS, Ecole Normale Supérieure, Paris, France.
[3]Now at Géosciences Rennes, CNRS, Université Rennes 1, Rennes, France.
[4]Department of Geosciences, National Taiwan University, Taipei, Taiwan.


0148-0227/07/2005JB004200$09.00

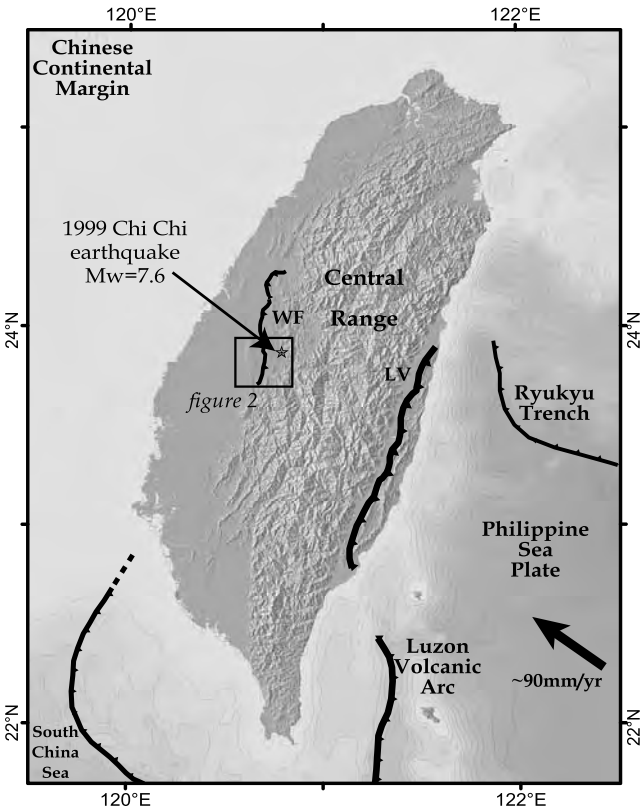


**Figure 1.** Geodynamical context of Taiwan. The convergence rate of ~90 mm/yr between the Philippine Sea Plate and the South China Block is taken after the GPS-derived plate kinematic model of *Sella et al.* [2002]. The Longitudinal Valley (LV) marks the suture between the two plates, and the Central Range (CR) of Taiwan develops to the west of this valley. Also indicated are the epicenter and the ~80 km long surface rupture of the September 1999 $M_w = 7.6$ Chi-Chi earthquake [*Ma et al.*, 1999]. The box locates the area represented on Figure 2 within the Western Foothills (WF) of central Taiwan.

ening is distributed to the active faults is still not clearly known, although balanced cross sections indicate that most of this shortening has been in fact taken up within the WF [*Simoes and Avouac*, 2006]. This information is key to assess seismic hazards in this highly populated area. Recently, based on the kinematic analysis of the Pakuashan fault tip fold at the deformation front of the range (Figures 2 and 3), *Simoes et al.* [2007] propose that deformation associated with the Changhua blind thrust has accommodated a shortening rate of 16.3 ± 4.1 mm/yr since initiation of fold growth, ~62 kyr ago. However, the contribution of the remaining active structures to the long-term crustal shortening across the WF and the Taiwanese range, integrated over several seismic cycles, is not yet resolved [e.g., *Cattin et al.*, 2004].

[3] The Chelungpu thrust is one of the major faults present within the WF of central Taiwan (Figures 2 and 3). Despite the several investigations that have taken place since the Chi-Chi earthquake, the slip rate on this thrust is still not well constrained. Balanced cross sections [*Yue et al.*, 2005] and estimates of the amount of erosion of the thrust sheet [*Simoes and Avouac*, 2006] indicate a total finite shortening of ~18.5–24.1 km. Studies of deposits incorporated into the thrust sheet suggest that fault inception is younger than 0.9 Ma [*Chen et al.*, 2001] and most probably as young as 0.7 Ma [*Chen et al.*, 2000]. This implies an average long-term shortening rate of ~26.4–34.4 mm/yr since the fault initiated. How this estimate relates to the present slip rate on the fault, over timescales of ~10 kyr to ~100 kyr integrating several seismic cycles, is poorly known. Paleoseismic investigations across the Chelungpu fault suggest much lower slip rates of 4.97 to 8.5 mm/yr over the last ~1.9 kyr [*W.-S. Chen et al.*, 2004a; *Wang*, 2005]. This rate may not be representative of the actual average slip rate because the time covered by these data may be too short in view of the probable return period of large earthquakes on this fault, estimated to ~630 to 1900 years from paleoseismology [*Wang*, 2005]. Also, this return period may not be regular. Morphotectonic investigations may therefore prove more appropriate to assess slip rates integrating several seismic cycles of the fault [e.g., *Lave and Avouac*, 2000]. Although *Chen et al.* [2003] recognize and date several fluvial deposits deformed by the Chelungpu thrust, such investigations have not yet been carefully performed on this structure.

[4] For this purpose, we conducted field investigations along a tributary to the Choushui Hsi, the Dungpuna river (Figures 2 and 5), where a strath terrace buried under a fill deposit provides a key geomorphic marker deformed by the Chelungpu and Chushiang thrust faults. Hereafter we first review the subsurface geometry of these faults, which can be constrained from field measurements and available seismic profiles in the nearby Choushui valley [*Wang et al.*, 2002] (Figures 2 and 5). On the basis of the deformed geometry of the surveyed strath terrace as well as on the age of this geomorphic marker, we derive slip rates on the Chelungpu and Chushiang faults over a period of ~11 kyr. Our results indicate that the Chelungpu thrust plays a major role in accommodating shortening across the Taiwanese range. Finally, we discuss our findings and their implications in terms of the seismic cycle of this active structure, as well as in terms of seismic hazards within the WF.

## 2. Structure of the Chelungpu and Chushiang Thrust Faults Along the Dungpuna River

[5] The Chelungpu and Chushiang thrust sheets consist of sediments that were initially deposited within the foreland basin (Figure 2). The Pliocene Chinshui Formation, characterized by thin shales and siltstones, is the most probable candidate for the decollement level of the Chelungpu fault [e.g., *Yue et al.*, 2005], as well as of the Chushiang thrust (Figure 3). It is overlain by the Upper Pliocene Cholan Formation, composed of light gray to brownish shales intercalated with fine to coarse sandy layers. These shallow marine sediments have been covered by the Pleistocene conglomeratic Toukoshan Formation mostly present west and north of our study area (Figure 2), and later by Quaternary fluvial deposits.

[6] In map view (Figure 2), although most of the main structures of west central Taiwan trend north-south and are consequently oblique to the main N20°E structural trend of the island (Figure 1), the Chushiang fault [*H.-W. Chen et al.*, 2004] strikes approximately N30°E (Figures 2 and 5), perpendicular to the direction of convergence and tectonic

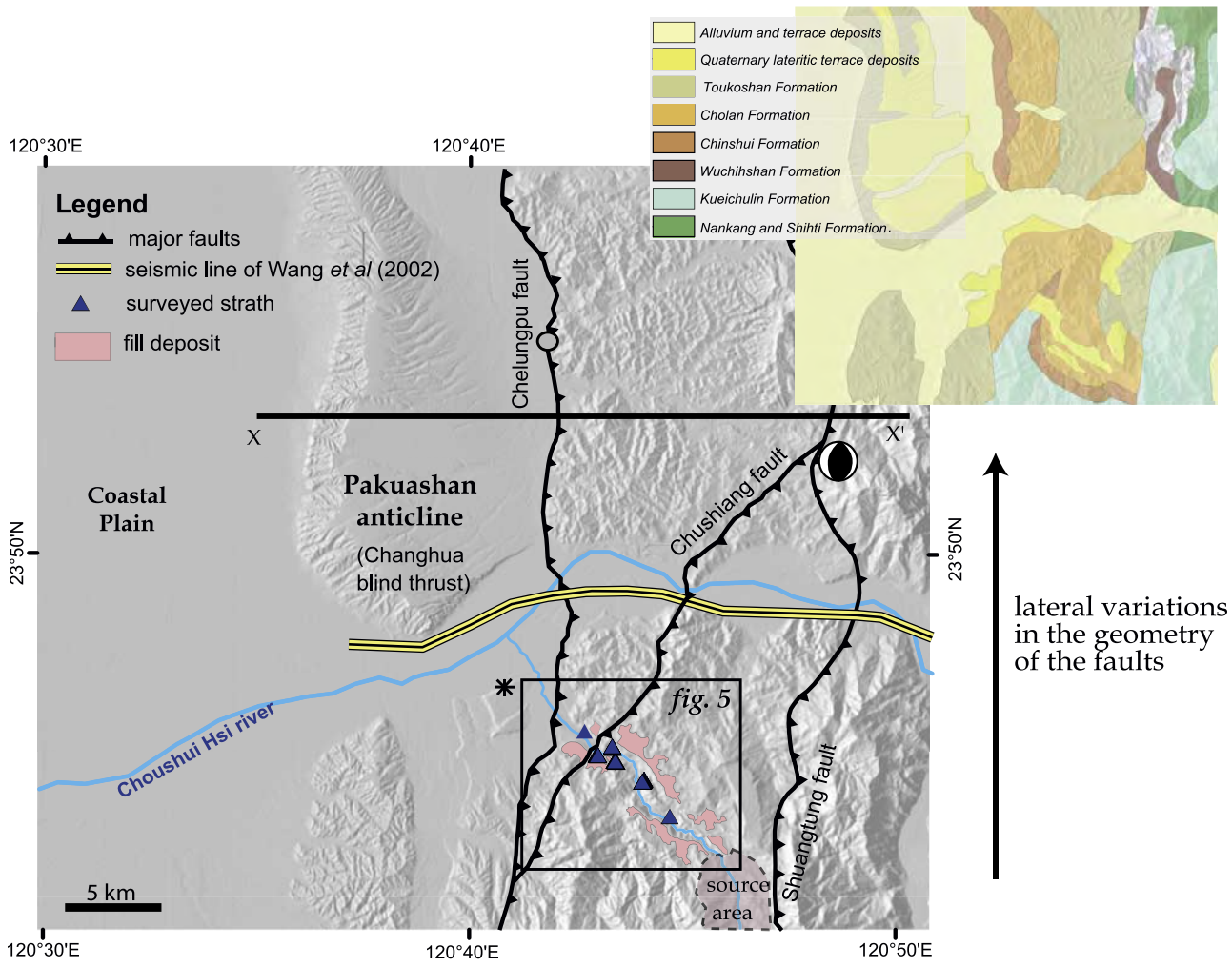


**Figure 2.** Map view of the structures within the WF of central Taiwan. The epicenter and the focal mechanism of the Chi-Chi earthquake (from the Central Weather Bureau) are shown. The Changhua blind thrust, which is related to the Pakuashan fault tip fold [*Simoes et al.*, 2007], marks the range front in this region. The position of the terrace, dated by *Ota et al.* [2002] to ~31 kyr B.P. and tilted by the Changhua fault, is also shown (asterisk). Gray circle locates the C3 borehole near the city of Nantou [*Streig et al.*, 2007]. The well analyzed by Chen et al. (submitted manuscript, 2006) in the Wufeng area is further north than the region represented here. Our study focuses on the Chelungpu and Chushiang faults in the area indicated by the box locating Figure 5 (see text for further details). Top right inset provides the geological map of the area.

transport [*Yu et al.*, 1997, 2003, 2001]. It connects the Chelungpu and Shuangtung thrusts (Figure 2) and it probably plays the role of a transfer fault. Structural measurements [e.g., *Yue et al.*, 2005; this study] and seismic investigations [*Wang et al.*, 2002] document the subsurface geometry of these structures. In the case of the seismic profile of *Wang et al.* [2002] further north along the Choushui river (Figure 3b), it can be noted that the velocities used for depth conversion are ~10–20% higher than those determined for the same formations in the region [*Chen*, 1978; *Sato et al.*, 1970], so that the depth of the imaged Chelungpu decollement coincided with that of the epicenter of the Chi-Chi earthquake [*Yue et al.*, 2005]. The seismic line shows that the Chelungpu and Chushiang thrust sheets can be interpreted as fault bend folds [e.g., *Suppe*, 1983], meaning that the thickness and length of the beds are preserved during deformation, and that internal deformation needed to accommodate the ramp geometry occurs by flexural bed-parallel slip. The Chushiang and Chelungpu faults appear to splay from a common ramp at ~3000 m depth (Figure 3b). A kink along this ramp is clearly imaged on the seismic profile where the faults connect at depth. It indicates that both the Chelungpu and the Chushiang faults are active, because such observed change in dip is expected if the slip transferred along the common ramp at depth is partitioned between the two faults emerging at the surface (Figure 3b) [e.g., *Simoes et al.*, 2007]. Recent activity on the Chushiang fault is also clearly supported by the presence of a fault scarp disrupting a fill terrace along the Dungpuna River (Figure 6). Further north along section X-X′ of Figure 2, this fault no longer exists and the decollement at depth merges at the surface as the single Chelungpu fault (Figure 3a). Along the Choushui river, the branch that links to

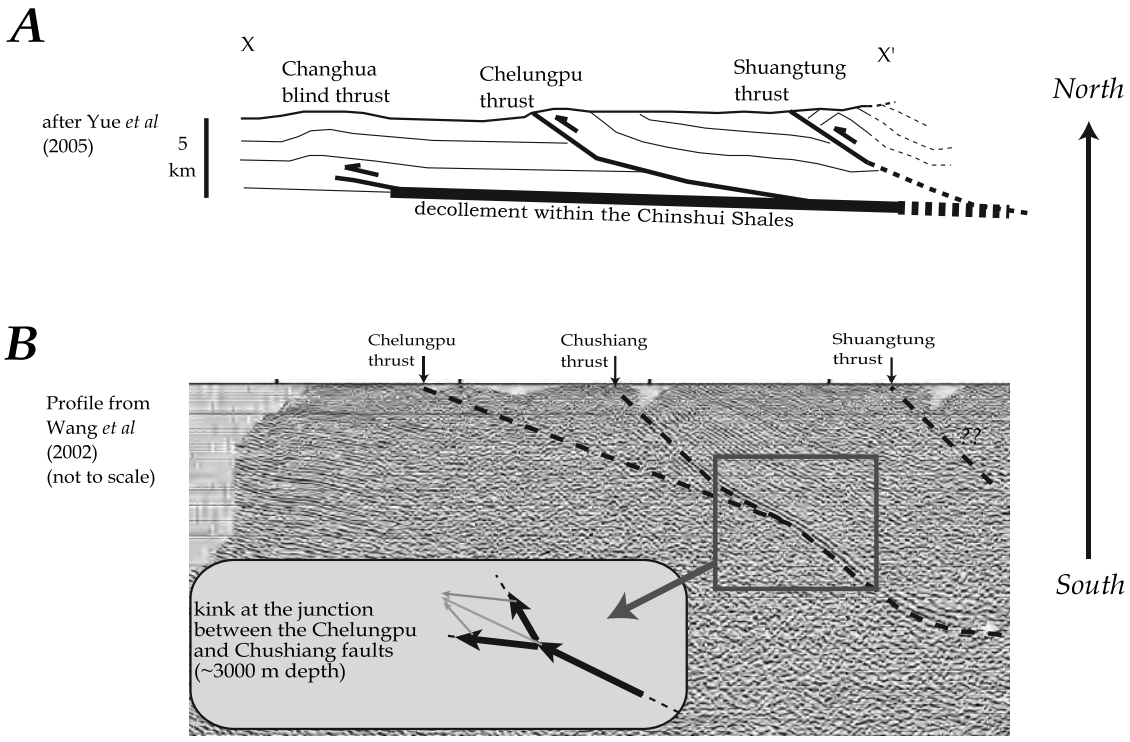


**Figure 3.** Geometry of the structures along two transects across the region shown in Figure 2. (a) To the north of the WF of central Taiwan, structures along the cross section X–X′ (Figure 2) show simple subsurface geometries [after *Yue et al.*, 2005]. (b) Further south, the seismic line of *Wang et al.* [2002] (not to scale) documents structures in the region investigated in this study (Figure 2). A kink where the Chelungpu and Chushiang thrusts connect indicates that slip on their common ramp at depth is partitioned on these two faults (schematic diagram in the inset). Therefore both of these structures are presently active. Note that in *Wang et al.*'s [2002] paper the Chushiang fault is named ''Tachienshan fault''. Here we use the name proposed in the revised geological map of *H.-W. Chen et al.* [2004].

the surface trace of the Chelungpu fault shows a dip angle of ~21°E on *Wang et al.*'s [2002] seismic profile, when corrected for the high velocities used for depth conversion. This fault dip angle differs from the greater dips observed for the layers on the seismic profile and retrieved from structural measurements along the Choushui river [*Yue et al.*, 2005]. In contrast, in our study area we measured apparent dip angles of ~20°E from sighting measurements on the hanging wall of the Chelungpu fault (Figure 5). In any case, the kink observed along the ramp at depth clearly indicates where the two faults merging at the surface connect (Figure 3b), so that, along with the surface fault trace, it provides a strong constraint on the Chelungpu fault dip angle. Structural measurements performed along the Choushui and Dungpuna rivers within the hanging wall of the Chushiang fault are consistent with the ~50°E dip observed on the seismic profile.

[7] Strike-and-dip measurements along the Dungpuna river (Figure 5) support a structural model (Figure 7b) that is consistent with the seismic profile of *Wang et al.* [2002] along the Choushui river. For the purpose of our subsequent analysis, we have chosen a N118E section, perpendicular to the Chushiang fault and to the strike directions measured in the field (Figures 5 and 7). Because the main strike of the Chelungpu thrust sheet is about north-south, projection of the 21°E dip deduced from *Wang et al.*'s [2002] east-west profile yields a 18°E dip angle along our cross section. In addition, the 3°E regional dip of the Changhua decollement projected on the N118E section has been retrieved from *Hung and Suppe*'s [2002] seismic investigations south of the Pakuashan anticline (Figure 2). The obtained cross section is used below to analyze the deformation of a geomorphic marker along the Dungpuna river.

## 3. Field Survey of the Terraces Observed Along the Dungpuna River

### 3.1. Description of the Terraces

[8] The Dungpuna river is a tributary to the Choushui river in the southernmost portion of the Chi-Chi earthquake surface rupture (Figure 2), and flows northwestward almost parallel to the direction of tectonic transport in Taiwan (Figure 5). Imbricate fluvial terraces are present in the hanging wall of the Chelungpu fault in the western part of our study area (Figures 5 and 7a). We were not able to find neither good outcrops exposing the geometry of the strath surfaces buried under these different terrace treads nor any datable material for age constraints. Upstream, the river has incised into a thick nonsorted fill deposit (Figures 5 and 7a). These sediments are typical of high-energy regimes alike debris flows: within the coarse-grained matrix, angular debris with varying diameters, often larger than 1 m, are common (Figure 8a). The coarse stratification suggests however that it was emplaced as a result of several episodes of deposition. Such thick deposit is not found regionally so that it is not

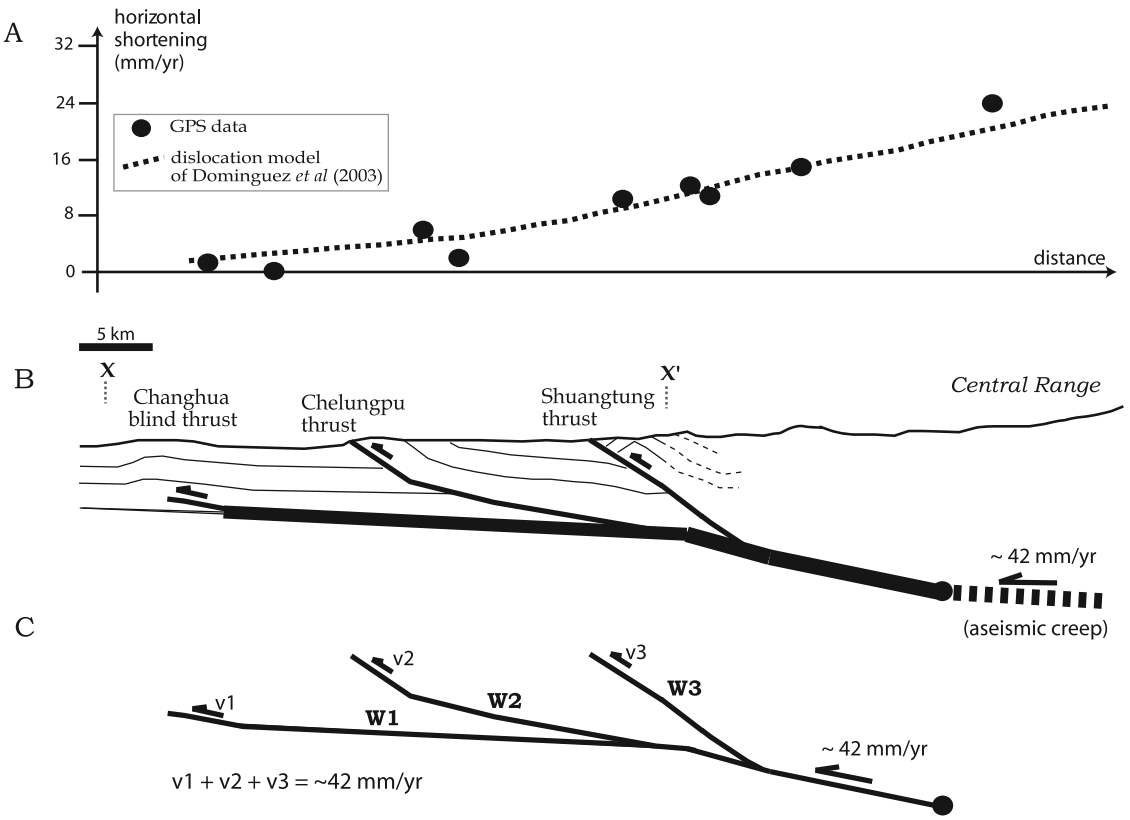


**Figure 4.** Active structures and cumulated strain across the WF of central Taiwan. (a) Interseismic GPS displacements in the WF (circles) relative to the Chinese continental margin (Figure 1), over the 5–6 years prior to the Chi-Chi earthquake [*Yu et al.*, 1997]. Also shown (dashed line) are horizontal displacements predicted at the surface by the elastic dislocation model of *Dominguez et al.* [2003] considering an aseismic creep rate of 40 mm/yr on the decollement beneath the CR (Figure 4b). (b) Cross section across central Taiwan, after *Yue et al.* [2005] along transect X–X′ (Figures 2 and 3a) for the foothills region and after the geometry of the best fitting creeping decollement of *Dominguez et al.* [2003] further east. The shortening rate of ~42 mm/yr across the Taiwanese range that is transferred to the active faults of the WF is after *Simoes and Avouac* [2006]. (c) Simplified geometry of the structures in Figure 4b used to calculate the seismic potency rate across the WF. Fault lengths $W_i$ are calculated from the fault tip down to the transition from seismic to aseismic slip given by the elastic model of *Dominguez et al.* [2003] (circle); $v_i$ represents slip rate on each fault. For simplicity, the transect at the latitude of section X–X′ (Figure 4b) is here considered rather than a transect further south incorporating the Chushiang fault.

necessarily linked to any particular climatic event. Its origin probably relates to local landslides, which are revealed further upstream by scars in the morphology of the valley walls (Figure 2). In the downstream area, this fill deposit has been disrupted by the Chushiang fault and clearly reveals a ~30–50 m high fault scarp (Figure 6).

[9] Deposition of this thick pile of sediments buried the former riverbed and preserved it as an erosive contact between the folded bedrock and the deposit (Figure 8b). This strath surface is presently visible along the steep valley walls in the westernmost portion of the hanging wall of the Chushiang thrust, revealing the amount of river incision that has occurred since this former riverbed was abandoned (Figures 7a). Upstream, this strath disappears beneath the active channel, and in this area the river still cuts into the fill deposit (Figures 5, 7a and 8a); this coincides with where bedrock dip angles become gentler (Figure 7b). This strath surface cannot be observed immediately downstream of the Chushiang fault scarp, in the hanging wall of the Chelungpu thrust. However, its location may still be constrained since it most certainly lies above the highest point where bedrock can be observed on the valley walls in this area, and beneath the top of the fill deposit. Immediately downstream of the Chelungpu fault trace, the former riverbed that lies in continuity with the surveyed strath surface has been buried under alluvial sediments (Figure 5). The profile of the deformed and incised strath terrace may be to first order compared to the presently active channel to retrieve incremental shortening on the Chelungpu and Chushiang faults [*Lave and Avouac*, 2000] (Figure 7a). The top of the deposit should not be used as a geomorphic marker of deformation since the initial geometry of such high-energy sediments may not be straightforward to assess (Figure 7a). Also, it is possible that this geometry is in fact time transgressive (*Weldon* [1986], as cited by *Bull* [1991]). Indeed, deposition of such thick pile of sediments could have occurred over a certain time lag.

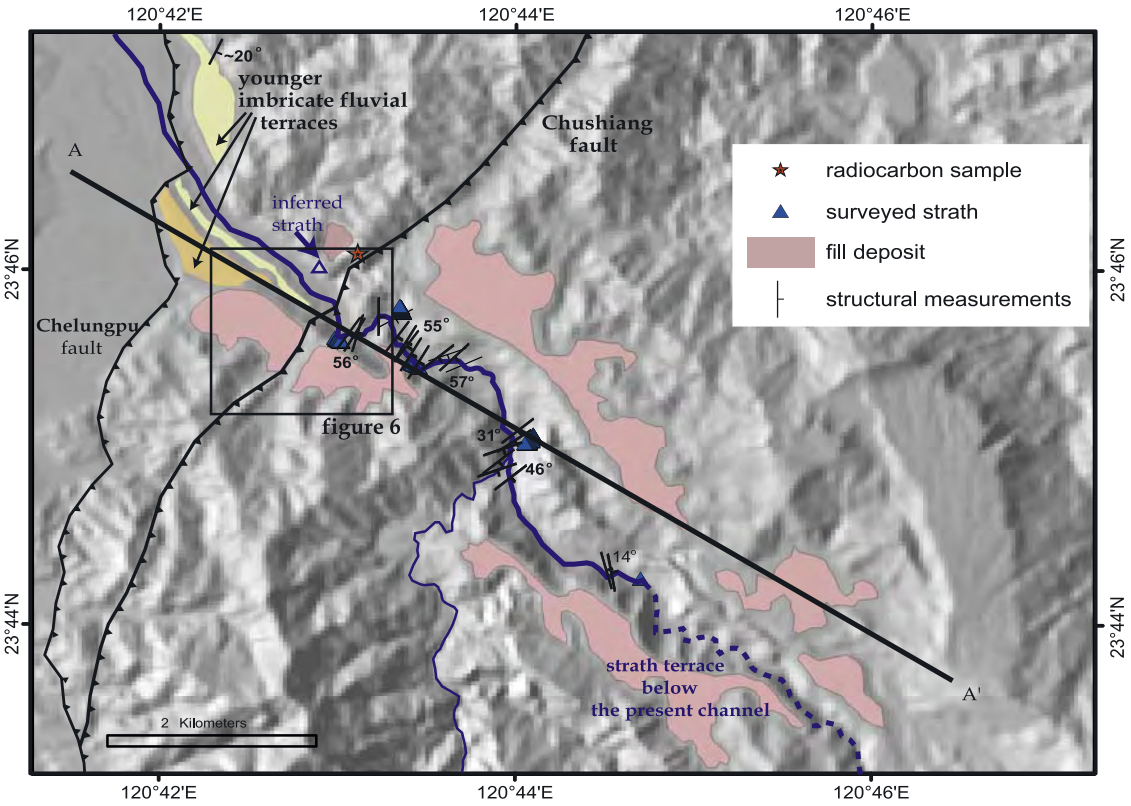


**Figure 5.** Area investigated along the Dungpuna river. The locations where the strath surface was surveyed in the field are shown (blue triangles); the strath inferred in the hanging wall of the Chelungpu fault is indicated by an open triangle. Upstream from our southeasternmost surveyed point, the strath disappears below the present channel (dashed blue line). The top of the fill deposit has been mapped only where its morphology could be clearly defined on the shaded DEM. Structural measurements were performed along the Dungpuna river valley. All data were projected on the N118E line A–A′ (Figure 7). Box locates the area detailed on Figure 6.

### 3.2. Retrieving the Geometry of the Deformed Strath Terrace and of the Fill Deposit

[10] To retrieve the position of the strath terrace surface, we used a ©Trimble 5700 RTK (Real-Time Kinematics) GPS system, equipped with a Trimble® Zephyr™ antenna (for more information on the system, see http://trl.trimble.com/docushare/dsweb/Get/Document-6785/5700WPertkE.pdf and http://trl.trimble.com/docushare/dsweb/Get/Document-140051/Spec_Sheet_-_R7_-_English.pdf). The RTK GPS system involves two units that are kept in radio contact during the whole experiment: a fixed base whose position is determined precisely initially, and a mobile rover. The position of the surveyed objects is then measured with the rover unit relative to the base station. These differential

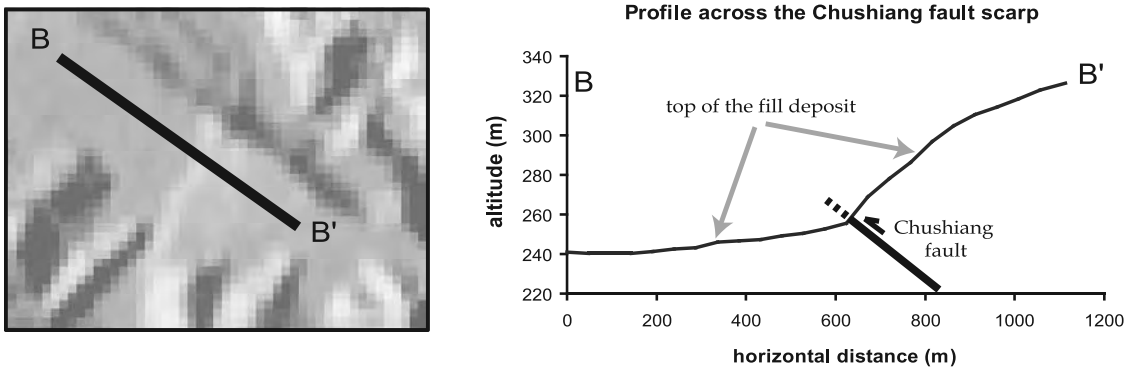


**Figure 6.** Chushiang fault scarp. This fault disrupts the fill deposit (Figure 5). (left) Shaded DEM clearly revealing the fault scarp in the morphology. (right) Topographic profile across the fault scarp (section B–B′).

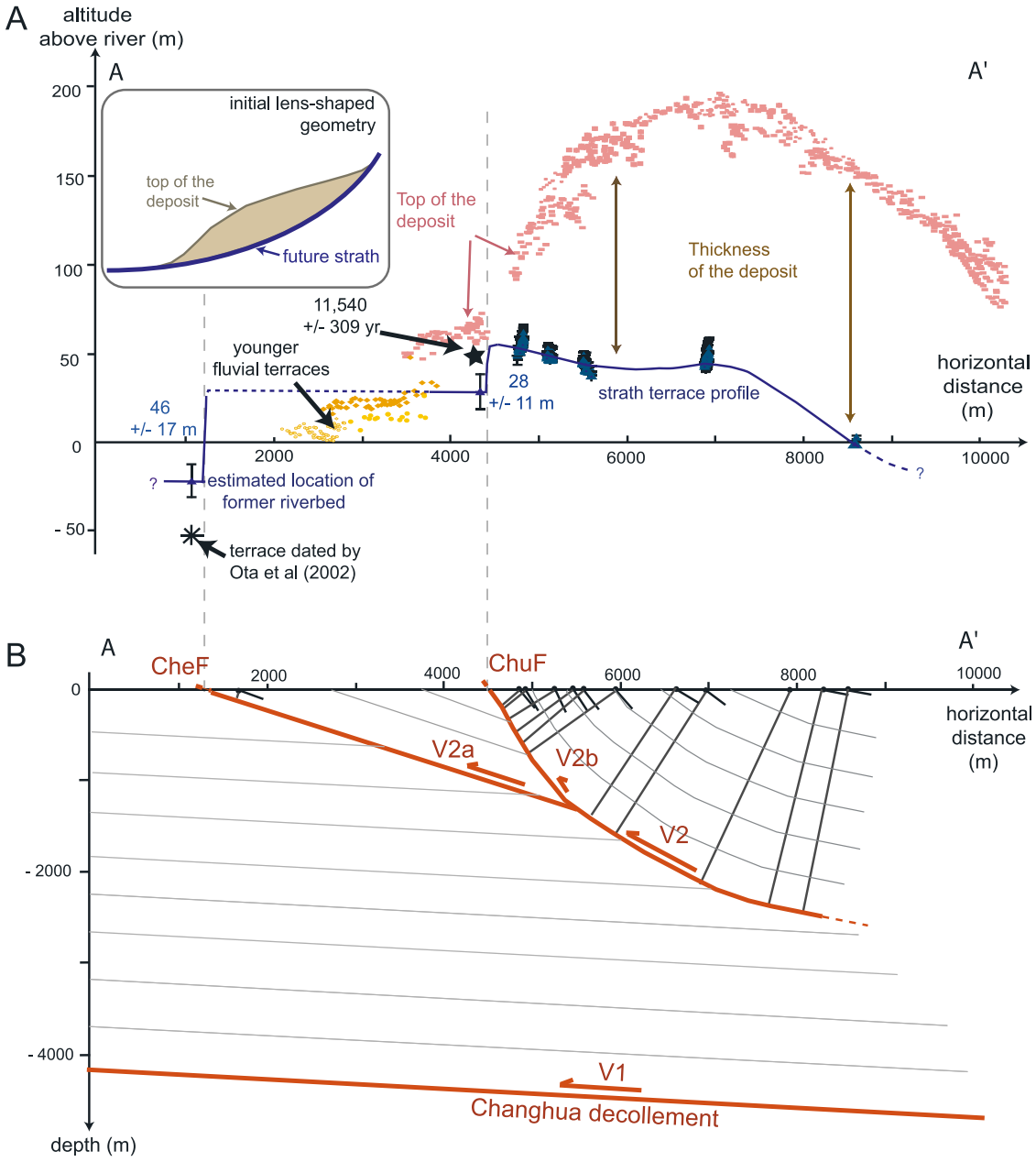


**Figure 7.** Structural and morphotectonic analysis of the strath terrace observed along the Dungpuna river. All data are shown projected onto line A–A′ (Figure 5). (a) Projection of the strath terrace (blue triangles) surveyed in the field and of the top of the fill deposit (pink dots) retrieved from the 40-m DEM (Figure 5). Altitudes are shown relative to the present active channel. Within the footwall of the Chelungpu fault, the position of the former riverbed in continuity with the strath further upstream is here only inferred and has not been observed in the field (see text for further details). The inferred position of the terrace dated by *Ota et al.* [2002] at this location is also shown (asterisk). Within the hanging wall of the Chushiang fault, the laterally varying thickness of the fill deposit suggests that it had an initial lens-shaped geometry, as illustrated schematically in top left inset. Location of the charcoal samples dated in this study is indicated (star). (b) Cross section across our study area based on structural measurements shown on Figure 5. Only locally averaged measurements are reported here and have been used to draw structures at depth. The Chelungpu (CheF) and Chushiang (ChuF) thrusts appear as splay faults branching onto a common decollement, whose total shortening rate, $V_2$, equals the sum of the rates on the two former faults, $V_{2a}$ and $V_{2b}$, respectively.

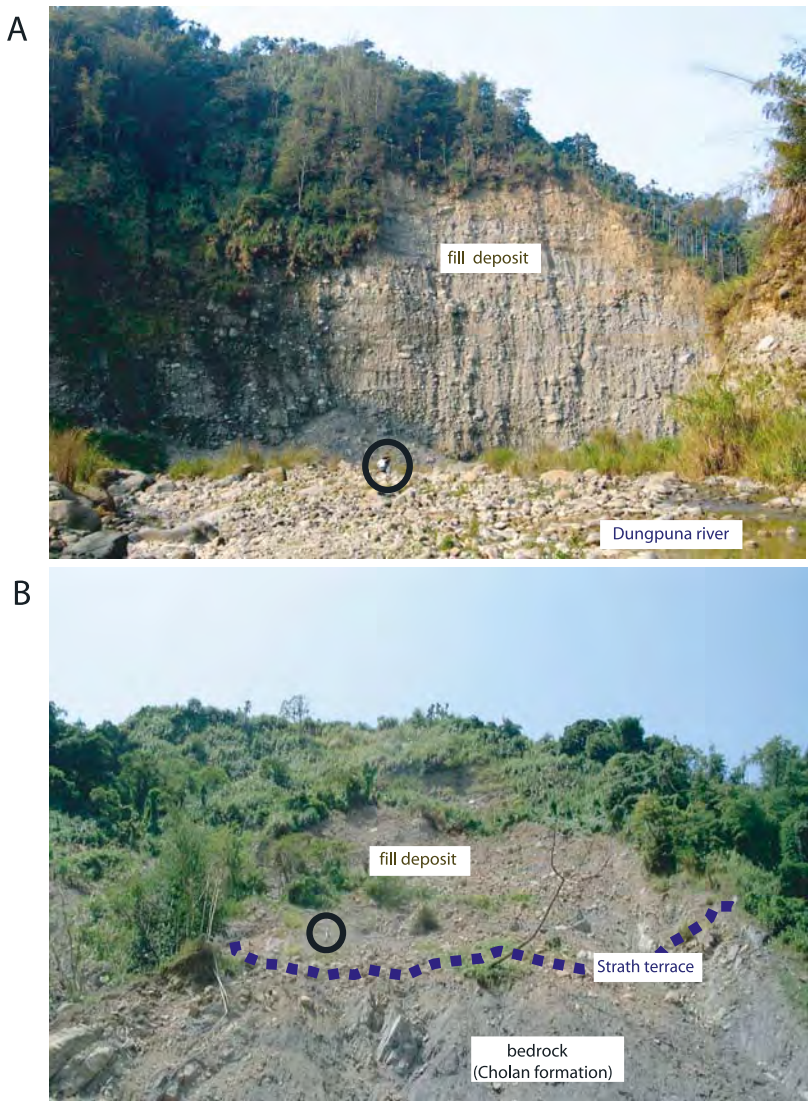


**Figure 8.** Field pictures of our survey along the Dungpuna river. Dark circles indicate people for scale. (a) Poorly sorted and coarse sediments of the Dungpuna fill deposit capping the strath terrace. Here the river still erodes into the deposit (Figure 5). (b) Example of outcrop where the strath terrace was surveyed. The strath (dashed line) appears to be an erosive contact between the folded bedrock and the coarse fill deposit.

measurements allow for very precise positions (with a precision usually of the order of 1 cm) since most of the errors inherent to GPS signals are corrected, except for multipath and receiver errors. Moreover, all measurements are tied to a unique consistent reference frame, which is most appropriate for our study. Since the strath surface along the steep valley walls could not be approached easily, a geodetic laser range distance meter (Advantage system from LaserAtlanta®; for more information, see http://www.laseratlanta.com/advantage.htm) equipped with a magnetic compass was coupled to our RTK GPS system to keep all measurements within this same reference frame. Distance, inclination and azimuth of the laser to the target were provided by the instrument and allowed calculation of the precise geometry of the deformed layers (Appendix A).

[11] The strath terrace can only be observed in the hanging wall of the Chushiang fault. Within the footwall of this fault, bedrock is observed as high as 16.6 m above the present riverbed, providing a lower limit of the position of the strath in this area. Field measurements are combined with a 40-m resolution digital elevation model (DEM), provided that measured altitudes are corrected to match those prescribed on the DEM for surveyed ground control points (ex: top of the deposit, present active river channel). The required vertical correction is found to be 36.5 ± 2.5 m. The top of the fill deposit and of the frontal imbricate fluvial terraces are directly extracted from the DEM (Figures 5 and 7a). The altitudes of the strath terrace and of the top of the deposit are given relative to the present active riverbed (Figure 7a). Indeed, this latter may provide a good approximation for the initial geometry of the deformed strath level, although changes in river gradient and sinuosity may have occurred since the strath was abandoned [*Lave and Avouac*, 2000]. For

**Table 1.** Radiocarbon Samples Collected From the Site Depicted in Figure 9[a]

| Sample | Material | Lab | Method | Conventional Age, years B.P. | Calibrated Age, cal years |
|---|---|---|---|---|---|
| 0606-A | charcoal | Lyon-2247(Poz) | AMS | 11,500 ± 100 | 11,540 ± 309 [11,231 to 11,850] |
| DPN-1 | charcoal | Lyon-2248(Poz) | AMS | 17,250 ± 180 | 18,580 ± 410 [18,170 to 18,990] |
| DPN-2 | charcoal | Lyon-2249(Poz) | AMS | 20,160 ± 270 | - |
| DPN-3 | charcoal | Lyon-2250(Poz) | AMS | 11,780 ± 100 | 11,821 ± 285 [11,536 to 12,107] |
| *Chen et al.* [2003][b] | Wood | NTU-3739 | Conv. | 11,590 ± 60 | 13,585 ± 265[b] |

[a]Calibration was performed after *Stuiver et al.* [1998]. For each sample, the range of acceptable calibrated ages is given, as well as the average value that can be proposed from this range.

[b]Also reported is the sample from *Chen et al.* [2003], which was collected from the top of the deposit, within the hanging wall of the Chelungpu thrust. It was dated using conventional methods. The calibration is in this case after *Stuiver and Becker* [1993].

the purpose of our analysis, data are projected onto a N118E transect perpendicular to the structures (Figures 5 and 7).

[12] To calculate uncertainties, we use a conservative approach detailed in Appendix A.

### 3.3. Age of Abandonment of the Strath Terrace

[13] Several radiocarbon samples within the fill deposit in the hanging wall of both the Chushiang and Chelungpu faults have been collected by *Chen et al.* [2002] and indicate ages of ~11,500 to 11,700 years B.P. (noncalibrated ages). The location of these samples and their stratigraphic position relative to the strath terrace is however not clearly reported. *Chen et al.* [2003] described a sample collected for radiocarbon dating close to the surface of the deposit on the hanging wall of the Chelungpu thrust. It yielded, before calibration, an age of 11,590 ± 60 years B.P. (Table 1). This age places an lower bound on the time of riverbed abandonment represented by the strath surface.

[14] We collected charcoal samples from silty layers within a colluvial wedge lying less than 4 m below the erosive base of the fill deposit in the footwall of the Chushiang fault (Figure 9). The wedge developed at the front of the fault and has been subsequently covered by the younger high-energy deposit. The basal erosive surface observed at this outcrop does not cut into the bedrock and stands ~30 m above the strath surveyed at this location. It thus most probably does not represent the former riverbed, but instead the contact between the fill deposit and the valley walls. The four samples collected yield calibrated ages from ~11,000 to ~20,000 calibrated (cal) years (calibration after *Stuiver et al.* [1998]; Table 1), but their respective stratigraphic positions do not appear to be consistent with the measured ages (Figure 9). We interpret the older ages to be from inherited charcoals. Youngest ages are thus most probably the closest to initiation of deposition of the fill deposit above the colluvial wedge. These values, which represent an upper limit to the age of

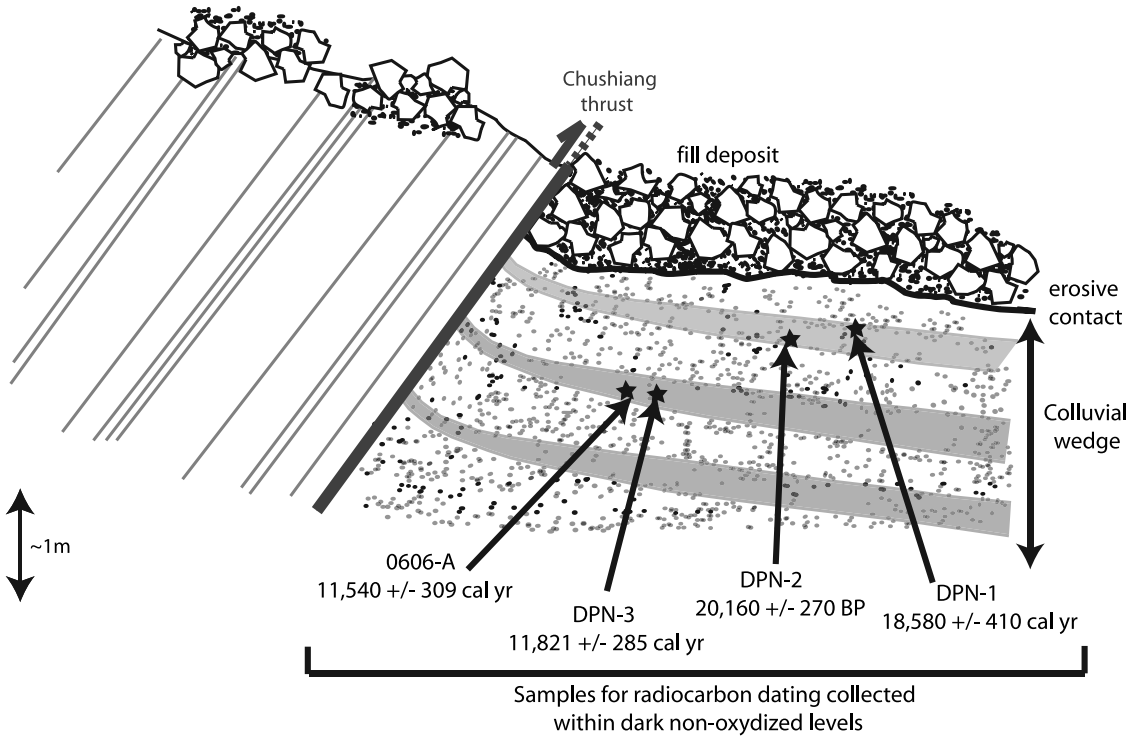


**Figure 9.** Schematic illustration of the site where four charcoal samples (0606-A, DPN-1, DPN-2, and DPN-3) were collected for radiocarbon dating. Ages and sample characteristics are presented in Table 1. These samples were retrieved from nonoxidized silt layers containing organic material, within a colluvial wedge at the front of the Chushiang fault (Figures 5 and 7a).

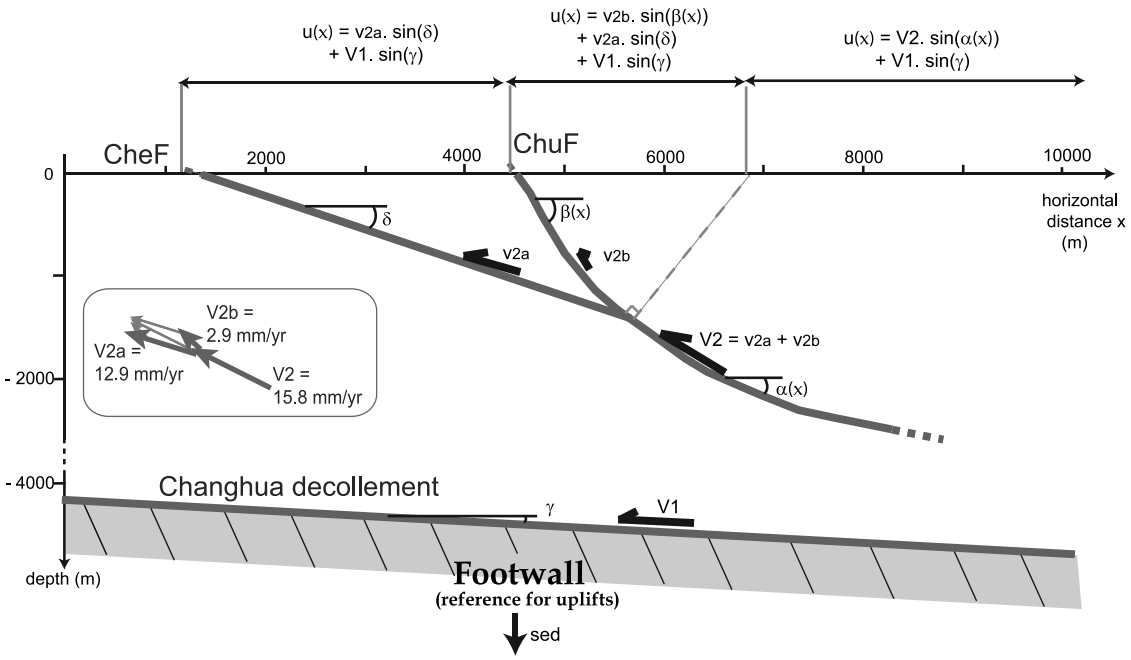


**Figure 10.** Model of the tectonic uplift rate $u$ expected along our field transect, based on the cross section of Figure 7b. Uplift is relative to the footwall, so that absolute uplift rates will have to account for sedimentation in the footwall, sed. Inset shows that slip rates obtained from our analysis of the strath terrace are compatible with the subsurface geometry inferred for the thrust faults.

strath abandonment, are close to the age retrieved by *Chen et al.* [2003] from the surface of the deposit and to those measured within the sediments by *Chen et al.* [2002], suggesting that deposition most probably occurred very rapidly although thicknesses of more than 100 m are observed (Figures 7a and 8a). Because of the similarity of all ages with those obtained in this study, we date riverbed abandonment represented by the strath terrace to the youngest age obtained from the colluvial wedge of Figure 9: 11,231 to 11,850 cal yr, as given from sample 0606-A. An average value of 11,540 ± 309 cal yr, spanning the whole time interval covered for this sample, is subsequently used (Table 1).

## 4. Slip Rates on the Chelungpu and Chushiang Faults

### 4.1. Approach

[15] Terraces may prove to be useful geomorphic markers in analyzing the kinematics of active structures if their initial geometries can be assessed. The initial depositional surface of a terrace tread may be particularly complex and not straightforward to define, particularly in the case of a high-energy deposit. Indeed, the sediment fill in our case study shows strong lateral variations in thickness, illustrated by varying differences in altitude between the top of the deposit and the basal strath surface (Figure 7a). Therefore, although the dome-shaped geometry of the top of the deposit likely records some incremental shortening associated with the Chushiang thrust, most of this observed pattern is the direct consequence of an initial lens-shaped depositional surface above the riverbed (Figures 7a). Our case study emphasizes the problems that might be encountered by using terrace treads for morphotectonic analyses of active structures. The strath surface proves more reliable because it can be compared directly to the present active riverbed as a first approximation [*Lave and Avouac*, 2000]. The present pattern of river incision revealed by the strath can be translated into incremental uplift after corrections for base level, river gradient and sinuosity changes [*Lave and Avouac*, 2000]. These latter two parameters may, however, not be easily assessed. Alternatively, such corrections can be avoided by using the pattern of differential incremental uplift within the hanging wall [*Thompson et al.*, 2002], or else the vertical throw across a fault scarp. This latter option is subsequently considered.

[16] A model of deformation is needed to retrieve incremental shortening across active structures from the pattern of uplift. The cross section of our study area suggests that the Chelungpu and Chushiang thrusts are mature faults (Figure 7b), so that a simple model of fault bend folding applies here. In this case, the uplift $u$ relative to the footwall, due to a displacement $d$ along the thrust fault, is simply expressed by

$$u = d\sin(\phi) \tag{1}$$

where $\phi$ is the apparent dip angle in the direction of thrusting [e.g., *Lave and Avouac*, 2000]. The footwall may be subsiding or rising, so that absolute uplift is only retrieved after correction for the vertical motion of the footwall. The proposed cross section of Figure 7b allows for defining precisely the expected contribution of the different structures at depth to the recorded tectonic uplift (Figure 10). The age constraints on strath abandonment subsequently allow for translation of the retrieved total incremental displacement $d$

into a shortening rate across the active structures. The method used to quantify errors on our estimated shortening rates is detailed in Appendix A.

### 4.2. Shortening Rates Across the Chushiang Fault

[17] We consider here the scarp of the Chushiang fault. In particular, to quantify the vertical throw of the strath terrace across the fault, the position of this geomorphic marker on both sides of the thrust has to be known. The strath has been surveyed in the hanging wall of the Chushiang fault (Figure 7a) but additional constraints on its location within the footwall are needed. This position can be assessed provided that the thickness of the fill deposit capping the strath terrace is known at this location. For this purpose, we first calculate the thickness of the sediments within the hanging wall of the Chushiang fault, by subtracting the altitude of the strath from the altitude of the top of the deposit. This estimate is only possible where the strath has been surveyed, between distances of ~4700 and ~7000 m along our section (Figure 7a). The retrieved thickness varies laterally, and can be fitted by a simple second-degree polynome. This pattern is then extrapolated further downstream to the immediate footwall of the Chushiang thrust where field observations indicate that the strath lies at least 16.6 m above the present riverbed. This approach suggests a thickness of 25 m at this location. With the top of the deposit at 61 m, the strath would be about 36 m above the present riverbed, consistent with field observations. However, the initial geometry of the fill may be more complex than the polynome derived above. In particular, the slope of the top of the deposit in the footwall of the Chushiang fault is significantly gentler than in the hanging wall (Figure 7a), so that the previous interpolation may largely underestimate the sediment thickness in the footwall block. By accounting for the minimum and maximum possible values of 16.6 and 36 m, respectively, we therefore consider that the strath lies at an average altitude of 26 ± 10 m above the present channel in this area.

[18] By comparing this position to the altitude of the strath in the hanging wall of the Chushiang fault, we estimate the vertical throw to 28 ± 11 m (Figure 7a). Taking into account the average 56°E dip observed at the front of the thrust from our field measurements, we get from equation (1) that 34 ± 18 m of horizontal displacement have been accommodated across the Chushiang thrust since the strath was abandoned. This in turn yields a shortening rate $V_{2b}$ (Figure 10) of 2.9 ± 1.6 mm/yr across this structure.

### 4.3. Shortening Rates on the Chelungpu Thrust

[19] The strath surface lies 26 ± 10 m above the present river in the hanging wall of the Chelungpu thrust, immediately west of the Chushiang fault (Figure 7a). Because the dip of the Chelungpu fault does not vary significantly along our section (Figures 3b and 7b), the amount of tectonic uplift of the strath is expected to be constant over the whole hanging wall of this thrust. Since the strath terrace was abandoned due to entrenchment of the Dungpuna river into the uplifted hanging wall of the Chelungpu fault, sedimentation has buried its downstream continuation on the footwall side of the Chelungpu fault. To determine the vertical throw across the fault scarp, we therefore need to estimate how much sedimentation has occurred over the last 11,540 ± 309 cal yr (sed in Figure 10). As reported by *Simoes and Avouac* [2006], Holocene subsidence rates of 2 to 3 mm/yr have been documented in the Coastal Plain west of the Pakuashan anticline [*Lai and Hsieh*, 2003], and are consistent with sedimentation rates offshore central Taiwan over a similar timescale [*Lee et al.*, 1993]. The effective sedimentation rate of the footwall of the Chelungpu fault just west of the fault scarp is probably less because of uplift related to slip along the Changhua fault and eventually also because of shortening and thickening of the sedimentary units forming the hanging wall of this most frontal fault (Figure 2). The kinematic analysis of *Simoes et al.* [2007] and available seismic profiles [*Hung and Suppe*, 2002; *Wang et al.*, 2002] across the southern Pakuashan anticline suggest that the backlimb of the fold does not extend as far east as the footwall of the Chelungpu thrust immediately west of the fault scarp. Therefore uplift due to thickening on the hanging wall of the Changhua fault is probably negligible in this area. The kinematics of the growing Pakuashan anticline has been relatively well constrained from the subsurface structure, the surface expression of the fold and from dated growth strata and indicates that the Changhua fault absorbs 16.3 ± 4.1 mm/yr of shortening [*Simoes et al.*, 2007]. Although the footwall of the Chelungpu fault closest to the fault scarp has not seen any uplift related to the growth of the Pakuashan fold, it is still uplifted by a small amount relative to the footwall of the Changhua fault due to the 3°E regional dip of the frontal blind thrust (Figure 10). This uplift is estimated to 0.8 ± 0.3 mm/yr based on the slip rate and on the dip of the fault. Vertical motion of the footwall of the Chelungpu fault since terrace abandonment (sed in Figure 10) has therefore been essentially driven by sedimentation of the foreland basin and we may therefore assume an effective sedimentation rate of 1.7 ± 0.9 mm/yr. This estimate is consistent with the probable position within the immediate footwall of the Chelungpu fault of the 31,950 years B.P. terrace dated by *Ota et al.* [2002] (Figure 2), constrained to a depth of ~53 m (Figure 7a) as predicted from the kinematic model of *Simoes et al.* [2007] corrected for the uplift related to the regional dip of the Changhua fault. Given the uncertainties on the proposed effective sedimentation rate, our result is also consistent with available constraints from wells and boreholes. Indeed, a sedimentation rate of 2 to 3 mm/yr over the last ~1.5 kyr has been retrieved from the C3 borehole near Nantou [*Streig et al.*, 2007] (Figure 2). In addition, over a time period of ~30 kyr, more comparable to that of our data, a lower rate of 0.91 mm/yr has been proposed from a well near Wufeng, 40 to 50 km north of our investigated area (Y.-G. Chen et al., Use of the optically stimulated luminescence method to date the sedimentary sequence in a trenching site on the source fault of the 1999 Chi-Chi earthquake, Taiwan, submitted to *Quaternary International*, 2006, hereinafter referred to as Chen et al., submitted manuscript, 2006). Therefore, on the basis of our analysis, we estimate that the 11,540 ± 309 cal yr old riverbed is now located 20 ± 12 m below the present channel within the footwall of the Chelungpu thrust fault (Figure 7a). Compared to our field observations in the hanging wall of the fault, this result yields a vertical throw of 46 ± 17 m across the fault scarp since the strath was abandoned. Because the Chelungpu thrust dips by 18°E in the study area (Figures 7b and 10), equation (1)

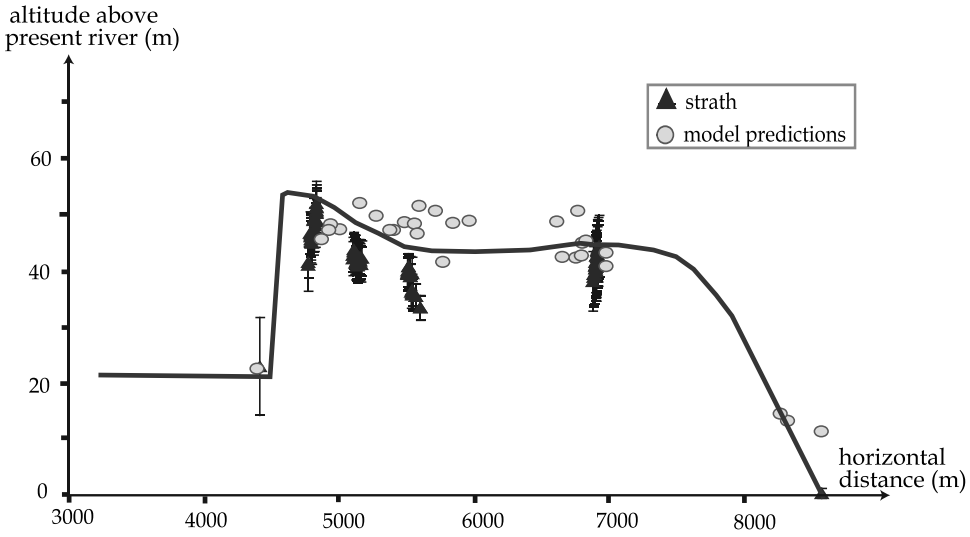


**Figure 11.** Profile of the strath terrace and rock uplift since the strath was abandoned, as predicted by the model of Figure 10 considering shortening rates of 12.8 and 2.9 mm/yr across the Chelungpu and Chushiang faults, respectively. Altitudes are given relative to the present riverbed. All structural measurements obtained in the field (Figure 5) were considered to calculate rock uplift: this explains the scatter of the model pattern. A sedimentation rate at the front of the system and a slip rate on the Changhua decollement of 2.5 and 16.3 mm/yr, respectively, are assumed to derive the absolute uplift.

indicates that 149 ± 55 m of shortening have been absorbed on the fault during the past ~11,540 years, which in turn yields a shortening rate of 12.9 ± 4.8 mm/yr.

### 4.4. Uplift Due to Slip on the Chelungpu and Chushiang Faults and River Incision

[20] Vertical displacements of the 11,540 ± 309 cal years old strath surface across the scarps of the Chelungpu and Chushiang faults allow for constraining the slip rates on these structures to 12.9 ± 4.8 and 2.9 ± 1.6 mm/yr, respectively. As suggested by the seismic profile of *Wang et al.* [2002] as well as our structural model (Figures 7b and 10), these two thrusts merge at depth into the same decollement level, which consequently accommodates a total shortening rate of 15.8 ± 5.1 mm/yr. We checked that these results and the partitioning of the 15.8 ± 5.1 mm/yr between the two shallower splay faults were consistent with the proposed subsurface geometry (inset in Figure 10).

[21] Finally, although river incision may not be directly related to tectonic uplift because some of the incision may have been associated with eventual hydrological changes [*Lave and Avouac*, 2000; *Poisson and Avouac*, 2004], we compare here the profile of the strath terrace to the pattern of vertical displacements predicted from the structural model of Figure 10 and using the shortening rates proposed above. The overall good fit supports our previous results (Figure 11). However, the structural model overestimates river incision at the distances of ~5000 to 5500 m along our section, possibly due to hydrological adjustments related to the confluence with a nearby tributary (Figure 5). The nontectonic contribution to the incision signal is probably not significant in our study area (Figure 11). In addition, we reconstructed the initial geometry of the fill deposit on either side of the Chushiang fault by correcting for the estimated vertical throw across this fault (Figure 12). A complex geometry, similar to the expected lens shape (Figure 7a), is obtained and supports our results. Also, this reconstruction clearly indicates that thicknesses predicted on the footwall of the Chushiang fault by simply extrapolating those observed further upstream can be significantly underestimated. Altogether, these results put credence to the idea that strath terraces can be used as accurate geomorphic markers for such morphotectonic investigations, provided that river adjustments in terms of gradient or sinuosity may be quantified.

## 5. Discussion

### 5.1. Partitioning of Shortening Across the Foothills and Implications for Seismic Hazards

[22] From the morphotectonic analysis of the strath terrace preserved along the Dungpuna river, to the south of the $M_w$ = 7.6 Chi-Chi earthquake rupture (Figure 2), we estimate shortening rates of 12.9 ± 4.8 and 2.9 ± 1.6 mm/yr on the Chelungpu and Chushiang faults, respectively. These two structures root at depth into a single ramp and decollement (Figures 7b and 10) that accommodate a total shortening rate of 15.8 ± 5.1 mm/yr. North of our field area, at the approximate latitude of the Chi-Chi earthquake epicenter, the Chushiang thrust disappears (Figures 2, 3a and 13). In this northern region of the WF of central Taiwan, the shortening rate absorbed by this structure is therefore probably transferred to other faults such as the Chelungpu or the Shuangtung faults. Transfer of slip to the Changhua fault is expected to be negligible because the kinematics of shortening of the Pakuashan anticline has been shown to be consistent from south to north [*Simoes et al.*, 2007]. These findings yield some crucial insights into assessing how shortening is partitioned and accommodated across the Taiwanese range.

[23] On the basis of the analysis of the foreland basin, *Simoes and Avouac* [2006] recently proposed that the long-term shortening rate across the range west of the suture zone (Figure 1) is of ~42 mm/yr. In addition, they showed from

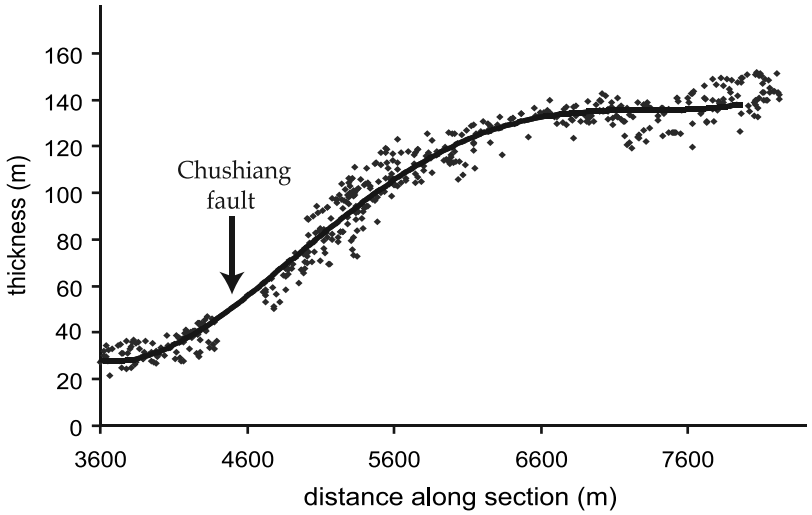


**Figure 12.** Reconstructed initial lens-shaped geometry of the fill deposit (dots). This geometry is calculated by subtracting the altitude of the strath from that of the top of the deposit and by accounting for the vertical throw across the Chushiang fault (Figure 10). This calculation is only performed where the strath terrace has been clearly identified in the field (Figure 7a) and does not extend upstream where the present river still incises into the fill. The data gap in the vicinity of the fault scarp is related to the fact that the top of the fill was not extracted from the DEM in this area (Figure 7a) because the scarp may have been affected by hillslope processes.

balanced cross sections across the WF that this shortening has been mostly (if not totally) absorbed across the foothills (Figure 4). If the ~16.3 mm/yr slip rate recently estimated on the Changhua fault [*Simoes et al.*, 2007] is combined with our results on the Chelungpu and Chushiang thrusts, a total of ~32 mm/yr appears to be accommodated on the most frontal structures. This in turn leaves ~10 mm/yr to be accommodated on more internal faults such as the Shuangtung fault, which is most probably presently active [*Sung et al.*, 2000]. Whether or not all the slip on these most frontal thrust faults is released seismically, in earthquakes such as the $M_w = 7.6$ Chi-Chi event, is an issue of major importance in evaluating the seismic hazards in west central Taiwan. Some insights can be obtained by estimating the potency rate (integral of the slip rate over the fault area) of the active structures present in this area, and by comparing it to the potency (integral of the coseismic slip over the ruptured fault area) during the 1999 Chi-Chi earthquake. Here we assume that slip rates and fault geometries do not vary significantly laterally within the study area, over a length of about 80 km from the southern to the northern ends of the Chi-Chi surface rupture. The potency rate $P$ in two dimensions across the foothills can be calculated from the product of the long-term slip rates $v_i$ and the downdip widths $W_i$ for each fault $i$:

$$P = \sum W_i v_i \tag{2}$$

The widths $W_i$ are taken over the whole length of each locked fault, from its surface trace to the tip of the aseismically creeping deep decollement (Figure 4c). The edge of the elastic dislocation inferred by *Dominguez et al.* [2003] to model interseismic deformation in west central Taiwan provides an estimate of the location of the downdip limit of the locked fault zone (Figure 4c). The geometry of the shallower structures is constrained from balanced cross sections along section X–X′ [*Yue et al.*, 2005] (Figure 3a). Two cases are considered, whether slip on the Chushiang fault is transferred to the Chelungpu fault ($P1$) or else to the Shuangtung fault ($P2$) in this area (Table 2). On the basis of the geometry proposed in Figure 4 and on the several estimates of the slip rates on the major faults (Table 2), we get for both cases a similar value of $\sim 3.40 \times 10^{-3}$ m$^2$/s for $P$. If all the strain accumulated across the foothills is released during major seismic events with the same potency as the 1999 Chi-Chi earthquake, we can then estimate the recurrence time of such events over the 80 km long stretch of the WF considered here. The geodetic moment $M_o$ of an earthquake is calculated as follows:

$$M_o = WLd\mu \tag{3}$$

where $W$, $L$ and $d$ are the downdip width and length of the ruptured area and the total displacement, respectively, and $\mu$ is the shear modulus. In the case of the Chi-Chi earthquake, $M_o$ has been estimated to $2.90 \times 10^{20}$ N m assuming a shear modulus of $3.3 \times 10^{10}$ N/m$^2$ [*Dominguez et al.*, 2003]. The released two-dimensional (2-D) potency, $P_{Chi\text{-}Chi}$, can then be calculated as $1.1 \times 10^5$ m$^2$ from

$$P_{Chi-Chi} = M_o/(L\mu) \tag{4}$$

By dividing $P_{Chi\text{-}Chi}$ by the rate $P$ determined above for the foothills, we get a recurrence time of ~62 to 64 years for events similar to the Chi-Chi earthquake. Historic seismicity reveals only one additional major seismic event in the area over the last 2 centuries, the 1848 $M \sim 7.1$ Changhua earthquake [*Tsai*, 1985]. This means that over the last two centuries the historic earthquakes have released a potency that is less than 50% of what would be required, on average over the long term, if all the locked faults were to slip only during large earthquakes. Given that seismicity in a given

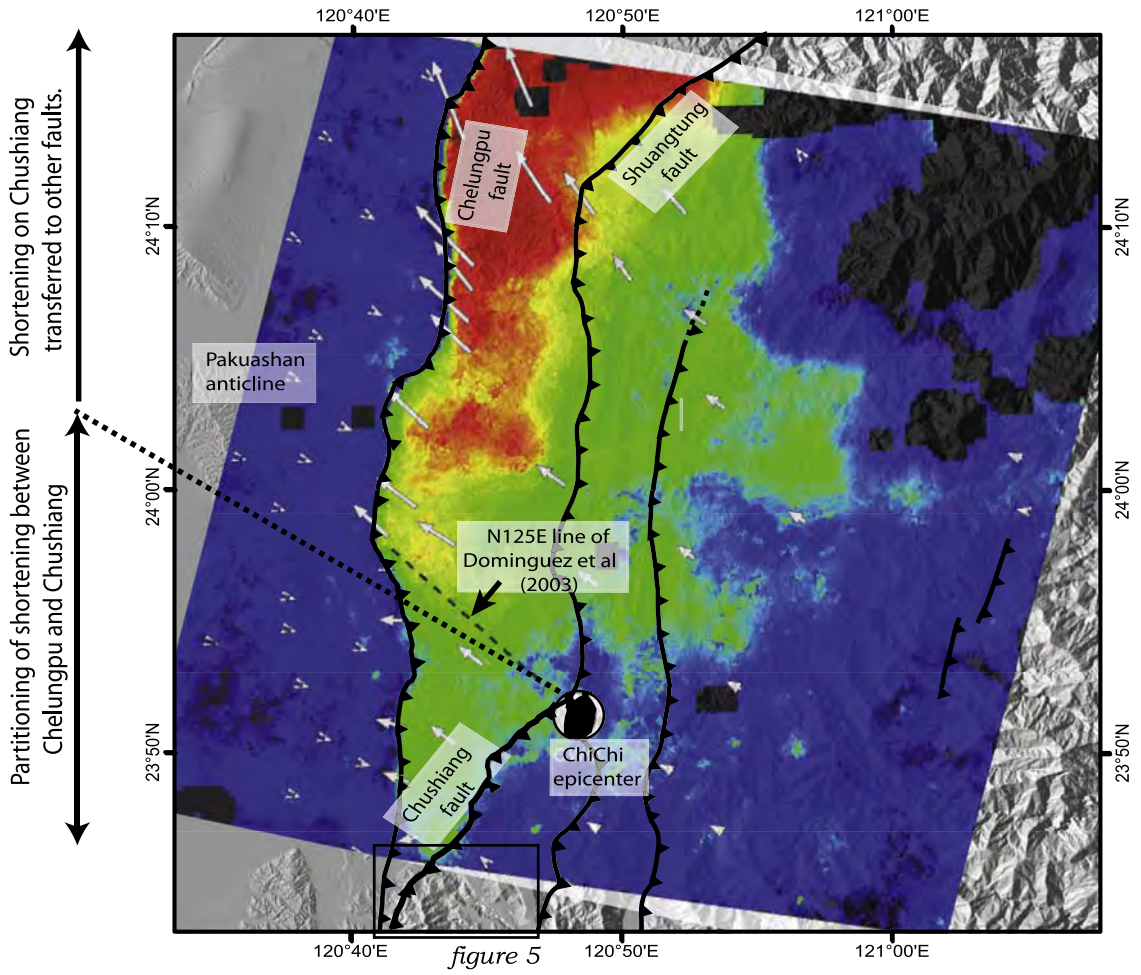


**Figure 13.** Horizontal coseismic slip distribution of the Chi-Chi earthquake retrieved from SPOT images [*Dominguez et al.*, 2003] and GPS data [*Yu et al.*, 2001] (white arrows) relative to the undeformed passive margin. Displacements from SPOT images range from 0 (blue) to 12 (red) m. The earthquake epicenter (from the Central Weather Bureau) coincides with the northern end of the Chushiang splay fault. Also shown is the N125°E line representing the sharp northward increase in coseismic displacements noted by *Dominguez et al.* [2003], which appears close to the N118°E projection in the direction of tectonic transport of the northward ending of the Chushiang fault (dashed line).

area generally obeys the Gutenberg-Richter law, with a *b* value of about 1, the contribution of earthquakes significantly smaller then the Chi-Chi earthquake (with a moment of less than say 7.0) is negligible. Aseismic slip could take up the fraction of the potency rate not expressed in seismicity. The negligible geodetic strain observed during the decade prior to the Chi-Chi earthquake [*Yu et al.*, 1997] (Figure 3a) suggests that this aseismic deformation would need to be episodic, with the possibility that a significant fraction could occur as afterslip during postseismic relaxation. Afterslip was indeed observed following the Chi-Chi earthquake [*Hsu et al.*, 2002], and found to have occurred over the portion of the fault that was previously locked. Afterslip contributed an additional potency of only about 10% of the coseismic potency over the three years following the earthquake. Given the decay rate of afterslip this mode of aseismic slip can explain only a fraction of the potency deficit. Also it has been observed that the Chi-Chi earthquake triggered some transient aseismic slip on the Changhua fault beneath Pakuashan [*Pathier et al.*, 2003]. However, the corresponding potency is negligible compared to that of the main shock. On the other hand these inferences rely on only two historic earthquakes which may not be representative of the whole seismic cycle in the WF. Another explanation might well be that the historical period has coincided with a period of seismic quiescence with a deficit of earthquakes compared to the long-term average. Paleoseismic investigations are required to address this question, in particular across the Shuangtung fault which has not yet been specifically studied. In any case the faults of the WF are a major source of seismic hazard in this heavily populated area.

### 5.2. Implications for the Chelungpu Fault in Terms of Along-Strike Variations in Slip Rate and Seismic Cycle

[24] Further north of our investigated area, the slip rate absorbed on the Chushiang thrust is expected to be transferred to the Chelungpu fault or to the Shuangtung fault (Figures 2 and 13), implying lateral north-south variations in the kinematics of these latter structures. Such transfer of

**Table 2.** Values of Downdip Width $W$ and Slip Rate $v$ of the Different Faults Used to Estimate the Seismic Potency Rate $P$ Across the Foothills of West Central Taiwan[a]

| | Changhua | Chelungpu | Shuangtung | $P$, $\times 10^{-3}$ m$^2$/s |
|---|---|---|---|---|
| $W$, km | 52.6 | 41.7 | 26.3 | |
| Case 1 $v$, mm/yr | 16 | 16 | 10 | 3.4 |
| Case 2 $v$, mm/yr | 16 | 13 | 13 | 3.3 |

[a]$W$ was evaluated based on the balanced cross section of Figure 3. Slip rates on the Changhua and Chelungpu faults are derived from *Simoes et al.* [2007] and this study, respectively. Two cases are here investigated, whether slip on the Chushiang fault is transferred to the Chelungpu fault (case 1) or to the Shuangtung fault (case 2) to the north of our study area. These shortening rates add up to the total ~42 mm/yr proposed by *Simoes and Avouac* [2006].

slip from the Chushiang fault to the other thrusts toward the north may be sharp or progressive. Further along-strike morphotectonic investigations of the thrust faults in the WF of central Taiwan are needed to clarify the proposed lateral variations in the partitioning of shortening across this region. In the case of the Chelungpu fault, the slip rate is therefore of 12.9 ± 4.8 mm/yr to the south and may be of up to 15.8 ± 5.1 mm/yr toward the north.

[25] Although the slip distribution during the Chi-Chi earthquake may not be representative of the behavior of the Chelungpu fault over a longer term, some insights into the seismic cycle of this thrust might be gained by comparing the coseismic slip distribution to the active structures in the WF, and to their partitioning of shortening. Indeed, sharp gradients in the horizontal coseismic slip distribution were observed in the southern area from the analysis of SPOT images [*Dominguez et al.*, 2003], along an approximately N125°E trending line initiating in the vicinity of the epicenter (Figure 13). This was interpreted as an eventual tear fault that has not yet reached the surface, and *Dominguez et al.* [2003] proposed that the earthquake originated in some complexity of the Chelungpu fault. Interestingly, the epicenter of the Chi-Chi earthquake lies in the area where, in map view, the Chushiang thrust connects to the Shuangtung fault and disappears to the north (Figure 13). Complexities in the coseismic slip distribution can thus be linked to the geometry of the structures along strike, and may be correlated to the lateral partitioning of long-term shortening. Also, the approximately N125°E trending gradient in coseismic displacements, subparallel to the approximately N118°E direction of tectonic transport in Taiwan and of slip during the Chi-Chi earthquake [*Dominguez et al.*, 2003; *Yu et al.*, 2001], coincides with where the Chushiang fault is expected to transfer its long-term shortening to the other faults of the WF (Figure 13). Because this region coincides with an increase in the horizontal coseismic slip along the Chelungpu fault, it can be proposed that slip on the Chushiang fault is actually taken up to the north mostly on the Chelungpu thrust rather than on the Shuangtung fault. However, how this coseismic pattern is valid over several seismic cycles and how it compares to the longer-term partitioning of slip is not straightforward. Also, such scenario implies the existence over the long-term of a major left-lateral tear fault at the northern termination of the Chushiang fault (Figure 13), which is not revealed in the morphology (Figure 2).

### 5.3. Comparison With the Previously Proposed Short- and Long-Term Slip Rates on the Chelungpu Fault and Implications

[26] The proposed slip rates on the Chelungpu thrust of 12.9 ± 4.8 mm/yr to the south and of up to 15.8 ± 5.1 mm/yr to the north are much higher than the 4.97–8.5 mm/yr values previously inferred over the last 1,900 years from trenches across the surface trace of the fault [e.g., *W. Chen et al.*, 2004b; *Wang*, 2005]. However, as reported by *W.-S. Chen et al.* [2004a], surface ruptures observed by trenching show a very complex pattern, with distributed shear at the surface break of the fault, so that displacements may not be straightforward to retrieve. Off-fault deformation within the thrust sheet may not account for the discrepancy between the two rates, because this deformation has been seen to be minor during the Chi-Chi earthquake [*Dominguez et al.*, 2003]. Also, although aseismic creep and minor seismic events contribute to accommodating shortening, they may not be recorded at the fault scarp and thus not have any recognizable signature for paleoseismic investigations. Finally, the seismic behavior of the Chelungpu fault may not be linear and steady in time, in which case the lower paleoseismic results indicate a period of seismic quiescence. These two different results deal with different timescales and may not be properly comparable.

[27] On the basis of sedimentologic arguments, *Chen et al.* [2000] proposed that activity on the Chelungpu fault began by 0.7 Ma. When compared to the finite shortening of ~18.5–24.1 km retrieved from balanced cross sections [e.g., *Yue et al.*, 2005] corrected for erosion of the thrust sheet [*Simoes and Avouac*, 2006], this implies a long-term shortening rate of ~26.4 to 34.4 mm/yr across the Chelungpu fault [*Simoes and Avouac*, 2006], higher than the maximum ~15.8 mm/yr proposed in this study over ~11,540 years. As suggested above, the behavior of the fault might not have been steady since it initiated, and slip rates may have slowed down over time. One possible explanation for the inconsistency between these rates taken at two different timescales is that some rearrangements occurred within the WF ~62 kyr ago, when shortening was transferred westward to the incipient Changhua fault [*Simoes et al.*, 2007]. Such westward transfer of deformation may have lowered the slip rate on the Chelungpu fault. This scenario is supported by the fact that the present slip rates on the two most frontal faults add together to the ~30 mm/yr total long-term shortening rate across the Chelungpu thrust sheet. Investigating deformed geomorphic markers older than 62 kyr in this frontal region would be most useful to test this hypothesis.

### 5.4. Using Strath Terraces for Morphotectonic Investigations

[28] Apart from these contributions to better constraining the kinematics of shortening across Taiwan, as well as the seismic hazards in the highly populated area of the WF, our study of the Dungpuna strath terrace also illustrates the importance of defining precisely the geomorphic marker to use for such morphotectonic investigations. *Weldon* [1986] (as cited by *Bull* [1991]) showed that large fluvial deposits might be time transgressive, so that their tops may not represent a deformed isochronous geomorphic marker. In addition to that, our investigations of the deposit in the Dungpuna valley indicate that the initial geometry of the

top of the deposit may be too complex to be precisely retrieved (Figure 12). The strath surface appears to be a more reliable geomorphic marker because it might be compared to the present active channel, provided that nontectonic contributions to river incision (changes in river gradient and sinuosity) may be quantified [e.g., *Lave and Avouac*, 2000]. The proposed slip rates on the Chushiang and Chelungpu faults have been retrieved from vertical throws across fault scarps and are thus independent of such hydrological changes.

## 6. Conclusion

[29] The morphotectonic study of the deformed strath terrace that was abandoned 11,540 ± 309 cal yr ago along the Dungpuna river, west central Taiwan, allows for estimating the slip rates on the Chelungpu and Chushiang faults to 12.9 ± 4.8 and 2.9 ± 1.6 mm/yr, respectively. In our study area, these two structures are splay faults branching at depth onto a common decollement, which consequently absorbs 15.8 ± 5.1 mm/yr of shortening. Lateral variations in the partitioning of shortening across the WF are expected because of the varying geometries of the thrust sheets. To the north of our study area, the slip rate on the Chelungpu fault may be possibly as high as the 15.8 ± 5.1 mm/yr derived for the decollement common to the two splay faults investigated here. Further studies are still needed to assess in more detail these probable lateral variations, but the proposed scenario correlates well with the distribution of horizontal coseismic slip during the Chi-Chi earthquake. In addition, this study provides clues for better assessing seismic hazards in this highly populated area of Taiwan. Indeed, some of the shortening absorbed across this western frontal part of the range could be released by aseismic creep, postseismic deformation or else small to intermediate earthquakes rather than by only major seismic events such as the $M_w$ = 7.6 Chi-Chi.

## Appendix A: Uncertainties on the Positions of the Strath and on the Calculated Slip Rates

[30] Uncertainties on the positions of each point measured by the RTK GPS are provided by the system and correspond to a 95% confidence level. They are of 1 cm + 1 ppm of the signal RMS in the horizontal direction, and of 2cm + 1ppm of the signal RMS in the vertical direction. In the case of distant targets, errors associated with the laser system were added to the RTK position of the laser base by using partial derivatives. Uncertainties on the slope distance are of the order of 3 to 5 cm but we use a value of 15 cm in our calculations because field work was performed during the wet season. Accuracies of the inclinometer and of the magnetic compass are 0.4 and 0.3°, respectively. Because the laser height was measured by a meter stick, we assume a maximum uncertainty of 2.5 mm (half a graduation). Finally, transposing these measurements into the DEM reference frame generates an additional vertical error of 2.54 m, derived from the dispersion in the comparison of measured anchor points with their altitude on the DEM.

[31] Uncertainties on horizontal incremental displacements and slip rates were then calculated based on the uncertainties on the different parameters and measurements, in quadrature and using partial derivatives. We estimate that these uncertainties correspond to a 95% confidence level, although partial derivatives certainly overestimate calculated uncertainties.

[32] **Acknowledgments.** The authors thank O. Beyssac (CNRS-ENS, France), Y.-C. Chan (Academia Sinica, Taiwan), J.-C. Hu (NTU, Taiwan), and S. Bernard (ENS, France) for their valuable help and support in the field. The RTK GPS and laser-range systems that allowed for surveying the strath surface were kindly provided by the CEA (France), Academia Sinica (Taiwan), respectively. Constructive reviews by N. Lundberg and A. Densmore and by Associate Editor J. Dolan helped improve this manuscript. These investigations were initiated thanks to a grant to J.P.A. from CNRS/INSU (France). This study was also partly funded by the Gordon and Betty Moore Foundation. This is Caltech Tectonics Observatory contribution 44.

## References

Bonilla, M. G. (1975), A review of recently active faults in Taiwan, U.S. Geol. Surv. Open File Rep., 75-41.

Bonilla, M. G. (1999), A note on historic and Quaternary faults in western Taiwan, *U.S. Geol. Surv. Open File Rep., 99-447*.

Bull, W. (1991), *Geomorphic Response to Climate Change*, 326 pp., Oxford Univ. Press, New York.

Cattin, R., A. Loevenbruck, and X. Le Pichon (2004), Why does the co-seismic slip of the 1999 Chi-Chi (Taiwan) earthquake increase progressively northwestward on the plane of rupture?, *Tectonophysics*, *386*, 67–80.

Chen, H.-W., M.-M. Chen, and T.-S. Shih (2004), 1:50,000 geological map of Taiwan, sheet 24, Nantou, Cent. Geol. Surv. of Taiwan, Taipei, Taiwan.

Chen, J.-S. (1978), A comparative study of the refraction and reflection seismic data obtained on the Changhua plain to the Peikang Shelf, Taiwan, *Pet. Geol. Taiwan.*, *15*, 199–217.

Chen, W.-S., et al. (2000), The evolution of foreland basins in the western Taiwan: Evidence from the Plio-Pleistocene sequences, *Bull. Cent. Geol. Surv.*, *13*, 136–156.

Chen, W.-S., K. D. Ridgway, C.-S. Horng, Y.-G. Chen, K.-S. Shea, and M.-G. Yeh (2001), Stratigraphic architecture, magnetostratigraphy, and incised-valley systems of the Pliocene-Pleistocene collisional marine foreland basin of Taiwan, *Geol. Soc. Am. Bull.*, *113*, 1249–1271.

Chen, W.-S., K.-J. Lee, L.-S. Lee, D. J. Ponti, C. Prentice, Y.-G. Chen, H.-C. Chang, and Y.-H. Lee (2004a), Paleoseismology of the Chelungpu Fault during the past 1900 years, *Quat. Int.*, *115–116*, 167–176.

Chen, W., K. Lee, L. Lee, H. Yang, C. B. Yang, I. Yen, H. Chang, C. Lin, W. Lin, and T. Shih (2004b), Paleoseismology of the 1999 Chi-Chi earthquake rupture, central Taiwan, *Eos Trans. AGU*, *85*(47), Fall Meet. Suppl., Abstract T11D-1303.

Chen, Y.-G., J. B. H. Shyu, K. Y. Lai, Y. Wang, R.-Y. Chuang, and W.-S. Chen (2002), Deformed terraces and active structures: A case along Tungpuna river, Nantao, paper presented at Annual Meeting of the Geological Society of China, Beijing.

Chen, Y.-G., Y.-W. Chen, W.-S. Chen, J.-F. Zhang, H. Zhao, L.-P. Zhou, and S.-H. Li (2003), Preliminary results of long-term slip rates of 1 999 earthquake fault by luminescence and radiocarbon dating, *Quat. Sci. Rev.*, *22*, 1213–1221.

Dominguez, S., J. Avouac, and R. Michel (2003), Horizontal coseismic deformation of the 1999 Chi-Chi earthquake measured from SPOT satellite images: Implications for the seismic cycle along the western foothills of central Taiwan, *J. Geophys. Res.*, *108*(B2), 2083, doi:10.1029/2001JB000951.

Hsu, Y., N. Bechor, P. Segall, S. Yu, L. Kuo, and K. Ma (2002), Rapid afterslip following the 1999 Chi-Chi, Taiwan earthquake, *Geophys. Res. Lett.*, *29*(16), 1754, doi:10.1029/2002GL014967.

Hsu, Y.-J., M. Simons, S.-B. Yu, L.-C. Kuo, and H.-Y. Chen (2003), A two-dimensional dislocation model for interseismic deformation of the Taiwan mountain belt, *Earth Planet. Sci. Lett.*, *211*, 287–294.

Hung, J.-H., and J. Suppe (2002), Subsurface geometry of the Sani-Chelungpu faults and fold scarp formation in the 1999 Chi-Chi Taiwan earthquake, *Eos Trans. AGU*, *83*(47), Fall Meet. Suppl., Abstract T61B-1268.

Lai, T.-H., and M.-L. Hsieh (2003), Late-Quaternary vertical rock-movement rates of the coastal plains of Taiwan, paper presented at Geological Society of Taiwan Meeting, Taipei, Taiwan.

Lave, J., and J. P. Avouac (2000), Active folding of fluvial terraces across the Siwaliks Hills, Himalayas of central Nepal, *J. Geophys. Res.*, *105*, 5735–5770.

Lee, T., C.-F. You, and T.-K. Liu (1993), Model-dependent $^{10}$Be sedimentation rates for the Taiwan Strait and their tectonic significance, *Geology*, *21*, 423–426.

Loevenbruck, A., R. Cattin, X. Le Pichon, M.-L. Courty, and S.-B. Yu (2001), Seismic cycle in Taiwan derived from GPS measurements, *C. R. Acad. Sci.*, *333*, 57–64.

Ma, H. F., C. T. Lee, Y.-B. Tsai, T.-C. Shin, and J. Mori (1999), The Chi-Chi, Taiwan earthquake: Large surface displacements on an inland thrust fault, *Eos Trans. AGU*, *80*, 605–611.

Ota, Y., J. B. H. Shyu, Y.-G. Chen, and M.-L. Hsieh (2002), Deformation and age of fluvial terraces south of the Choushui river, central Taiwan, and their tectonic implications, *West. Pac. Earth Sci.*, *2*, 251–260.

Pathier, E., B. Fruneau, B. Deffontaines, J. Angelier, C. P. Chang, S.-B. Yu, and C.-T. Lee (2003), Coseismic displacements of the footwall of the Chelungpu fault caused by the 1999, Taiwan, Chi-Chi earthquake from InSAR and GPS data, *Earth Planet. Sci. Lett.*, *212*, 73–88.

Poisson, B., and J. P. Avouac (2004), Holocene hydrological changes inferred from alluvial stream entrenchment in north Tian Shan (northwestern China), *J. Geol.*, *112*, 231–249.

Sato, K., C. Y. Meng, J. Suyama, S. Kurihara, S. Kamata, H. Obayashi, E. Inoue, and P. T. Hsiao (1970), Reports on the seismic refraction survey on land in the western part of Taiwan, Republic of China, *Pet. Geol. Taiwan*, *7*, 281–293.

Sella, G. F., T. H. Dixon, and A. Mao (2002), REVEL: A model for Recent plate velocities from space geodesy, *J. Geophys. Res.*, *107*(B4), 2081, doi:10.1029/2000JB000033.

Shyu, J. B. H., K. Sieh, Y.-G. Chen, and C.-S. Liu (2005), Neotectonic architecture of Taiwan and its implications for future large earthquakes, *J. Geophys. Res.*, *110*, B08402, doi:10.1029/2004JB003251.

Simoes, M., and J. P. Avouac (2006), Investigating the kinematics of mountain building in Taiwan from the spatiotemporal evolution of the foreland basin and western foothills, *J. Geophys. Res.*, *111*, B10401, doi:10.1029/2005JB004209.

Simoes, M., J. P. Avouac, Y.-G. Chen, A. K. Singhvi, C. Y. Wang, J. M., Y.-C. Chan, and S. Bernard (2007), Kinematic analysis of the Pakuashan fault tip fold, west central Taiwan: Shortening rate and age of folding inception, *J. Geophys. Res.*, doi:10.1029/2005JB004149, in press.

Streig, A. R., et al. (2007), Evidence for prehistoric coseismic folding along the Tsaotun segment of the Chelungpu fault near Nantou, Taiwan, *J. Geophys. Res.*, doi:10.1029/2006JB004493, in press.

Stuiver, M., and B. Becker (1993), High-precision decadal calibration of the radiocarbon time scale, AD 1950–6000 BC, *Radiocarbon*, *35*, 35–65.

Stuiver, M., P. J. Reimer, and T. F. Braziunas (1998), High precision radiocarbon age calibration for terrestrial and marine samples, *Radiocarbon*, *40*, 1127–1151.

Sung, Q., Y.-C. Chen, H. Tsai, Y.-G. Chen, and W.-S. Chen (2000), Comparison study of the coseismic deformation of the 1999 Chi-Chi earthquake and long-term stream gradient changes along the Chelungpu fault in Central Taiwan, *Terr. Atmos. Ocean. Sci.*, *11*, 735–750.

Suppe, J. (1983), Geometry and kinematics of fault-bend folding, *Am. J. Sci.*, *283*, 684–721.

Thompson, S. C., R. J. Weldon, C. M. Rubin, K. Abdrakhmatov, P. Molnar, and G. W. Berger (2002), Late Quaternary slip rates across the central Tien Shan, Kyrgyzstan, central Asia, *J. Geophys. Res.*, *107*(B9), 2203, doi:10.1029/2001JB000596.

Tsai, Y.-B. (1985), A study of disastrous earthquakes in Taiwan, 1683–1895, *Bull. Inst. Earth Sci. Acad. Sin.*, *5*, 1–44.

Wang, C. Y., C.-L. Li, F.-C. Su, M.-T. Leu, M.-S. Wu, S.-H. Lai, and C.-C. Chern (2002), Structural mapping of the 1999 Chi-Chi earthquake fault, Taiwan, by seismic reflection methods, *Terr. Atmos. Ocean. Sci.*, *13*, 211–226.

Wang, J.-H. (2005), Earthquakes rupturing the Chelungpu fault in Taiwan are time predictable, *Geophys. Res. Lett.*, *32*, L06316, doi:10.1029/2004GL021884.

Weldon, R. J. (1986), Cenozoic geology of Cajon Pass: Implications for tectonics and sedimentation along the San Andreas fault, Ph.D. thesis, 400 pp, Calif. Inst. of Technol., Pasadena.

Yu, S.-B., H.-Y. Chen, and L.-C. Kuo (1997), Velocity field of GPS stations in the Taiwan area, *Tectonophysics*, *274*, 41–59.

Yu, S.-B., et al. (2001), Preseismic deformation and coseismic displacements associated with the 1999 Chi-Chi, Taiwan, earthquake, *Bull. Seismol. Soc. Am.*, *91*, 995–1012.

Yu, S., Y. Hsu, L. Kuo, H. Chen, and C. Liu (2003), GPS measurement of postseismic deformation following the 1999 Chi-Chi, Taiwan, earthquake, *J. Geophys. Res.*, *108*(B11), 2520, doi:10.1029/2003JB002396.

Yue, L.-F., J. Suppe, and J.-H. Hung (2005), Structural geology of a classic thrust belt earthquake: The 1999 Chi-Chi earthquake Taiwan ($M_w$ = 7.6), *J. Struct. Geol.*, *27*, 2058–2083.

J. P. Avouac, Tectonics Observatory, California Institute of Technology, MC 100-23, 1200 E. California Blvd., Pasadena, CA 91125, USA.

Y.-G. Chen, Department of Geosciences, National Taiwan University, P.O. Box 13-318, Taipei 106, Taiwan.

M. Simoes, Géosciences Rennes, Université Rennes 1, Campus Beaulieu, F-35042 Rennes, France. (martine.simoes@univ-rennes1.fr)